Soft Matter

Engineered Interaction Between Short Elastin-Like Peptides and Perfluorinated Sulfonic-acid Ionomer

Journal:	*Soft Matter*
Manuscript ID	SM-ART-02-2018-000351.R1
Article Type:	Paper
Date Submitted by the Author:	13-Apr-2018
Complete List of Authors:	Su, Zihang; Case Western Reserve University Case School of Engineering, Pramounmat, Nuttanit; Case Western Reserve University Case School of Engineering Watson, Skylar; university of arkansas Renner, Julie; Case Western Reserve University Case School of Engineering

Soft Matter

Paper

Engineered Interaction Between Short Elastin-Like Peptides and Perfluorinated Sulfonic-acid Ionomer

Received 00th Feburary 2018,
Accepted 00th March 2018

DOI: 10.1039/x0xx00000x

www.rsc.org/

Zihang Su,[a] Nuttanit Pramounmat,[a†] Skylar T. Watson [b†] and Julie N. Renner *[a]

Control of ionomer thin films on metal surfaces is important for a range of electrodes used in electrochemical applications. Engineered peptides have emerged as powerful tools in electrode assembly because binding sites and peptide structures can be modulated by changing the amino acid sequence. However, no studies have been conducted showing peptides can be engineered to interact with ionomers and metals simultaneously. In this study, we design a single-repeat elastin-like peptide to bind to gold using a cysteine residue, and bind to a perfluorinated sulfonic-acid ionomer called Nafion® using a lysine guest residue. Quartz crystal microbalance with dissipation monitoring and atomic force microscopy are used to show that an elastin-like peptide monolayer attached to gold facilitates the formation of a thin, phase-separated ionomer layer. Dynamic light scattering confirms that the interaction between the peptide with the lysine residue and the ionomer also happens in solution, and circular dichroism shows that the peptides maintain their secondary structures in the presence of ionomer. These results demonstrate that elastin-like peptides are promising tools for ionomer control in electrode engineering.

Introduction

Protein and peptide engineering is increasingly being utilized as a tool for electrode manufacturing in electrochemical fields, particularity for enzyme-based electrodes,[1-3] which are used as sensors, and as implantable power sources. Non-enzymatic electrodes have also been manufactured using engineered peptides as templates for metal formation, with applications in energy storage[4] and electrocatalysis.[5] While control of catalytic components (e.g. enzymes and metals) is important for electrochemical applications, ionic transport is also pivotal for the performance of many of these devices. Efficient ionic transport can be achieved by incorporating highly-charged, ion-conductive polymers called ionomers (a special kind of polyelectrolyte) in the electrode layers. However, challenges exist with controlling ionomer. In the case of enzymatic electrodes, ionic conduction is needed while enzymes also require shielding from regions of extreme pH that the ionomers help facilitate.[3] In the case of metal-based electrodes, increasing evidence suggests that control of ionomer-catalyst interactions is pivotal for efficient catalyst usage in electrochemical devices such as fuel cells.[6-8]

Control of ionomer film structures via casting with salts has shown promise for harboring enzymes in favorable pore structures for electrodes.[9-11] We propose to gain additional ionomer controllability by using a novel, tunable engineered peptide system based on elastin, which binds to both ionomer and metal to facilitate organization. Elastin-like peptide sequences are derived from the hydrophobic domain of tropoelastin and consist of a pentapeptide sequence of a repetitive VPGXG motif, where X is a guest residue that can be any amino acid other than proline.[12] By modifying the guest residues in elastin's pentapeptide sequences, the hydrophobicity of the molecules can be adjusted, and the temperature at which a dense coacervate forms can be tuned (known as the inverse transition temperature).[13] The transition temperature is also sensitive to elastin concentration and chain length,[14] as well as pH and salt content.[15] Elastin-like peptides are also known for having dynamic random coil and beta-turn structures, which change upon heating.[16] Elastin-based sequences are potentially attractive ionomer-organizing peptide sequences because they are highly tunable and environmentally responsive,[15] compatible with enzymes,[17] self-assemble into fibers,[18] micelles,[15] and nanopores,[19] and can be manufactured in large quantities.[20] If elastin could be engineered to interact with ionomer, elastin's unique properties could be utilized to template complex ionomer structures for different systems, and potentially engineered to respond to environmental stimuli in the future.

[a] Department of Chemical and Biomolecular Engineering, Case Western Reserve University, Cleveland, OH 44106
[b] Ralph E Martin Department of Chemical Engineering, University of Arkansas, AR 72701.
† Authors contributed equally to this paper
Electronic Supplementary Information (ESI) available: [details of any supplementary information available should be included here]. See DOI: 10.1039/x0xx00000x

Notably, elastin-like peptide has been used to template metals for efficient electrodes in battery applications.[18, 21-23] While examples of elastin-like peptide being manufactured with weak polyelectrolytes (e.g. poly (acrylic acid)[24] and poly(ethyleneimine)[25]) can be found in literature, no studies to date have utilized elastin-based sequences to control the ionomers commonly used in electrochemical applications. One of the most ubiquitous ionomers in industrial electrochemical devices (e.g. fuel cells and electrolyzes) is Nafion®,[26] and is therefore chosen for this study. The chemical structure of Nafion® consists of a perfluorinated backbone with perfluoroether side chains terminated with sulfonic acid groups tethered throughout the polymer, and thus is called a perfluorinated sulfonic-acid (PFSA) polymer. The presence of the backbone and the sulfonic acid groups causes the material to naturally phase separate, which facilitates proton conduction via the covalently attached ionic groups.

We seek to design elastin-like peptides which bind to Nafion® ionomer via ionic crosslinking with the guest residues. Ionic crosslinking has been utilized in other composite Nafion® materials,[27, 28] but not with proteins. This study therefore has two main objectives. First, we demonstrate that elastin-like peptides can be engineered to bind with Nafion® in an aqueous environment. To our knowledge, this is the first study that shows such an interaction occurs. Binding is studied in solution as well as when peptides are immobilized to a metal surface. Gold (Au) is utilized as a model metal surface in this study. The second objective is to characterize the ionomer layers that form on the metal surfaces facilitated by the peptide anchor. We characterize molar ratios of peptide bound to acid groups within the ionomer, and also provide a comparison of length scales across characterization techniques. Overall, the goal of this study is to show that engineered elastin-like peptides can serve as promising tools to control ionomer.

Experimental methods

Materials

Deionized (DI) water was used in all experiments, and obtained using a mixed bed deionizer tank from Western Reserve Water Systems (1-10 megohm). Nitrogen (N_2, 99.99%) gas, used for drying, was obtained for Airgas. Ammonium hydroxide solution (NH_4OH, 30%) was purchased from Alfa Aesar. Sodium dodecyl sulfate ($C_{12}H_{25}NaO_4S$, 99%) was purchased from Hoefer. Hydrogen peroxide solution (H_2O_2, 25%) and Nafion® perfluorinated resin, aqueous dispersion (10 wt.% in H_2O), were purchased from Sigma-Aldrich.

Table 1: Design of elastin-like peptides used in this study.

Peptide Sequence	Description	Guest Residue	Molecular Weight (g/mol)
Ac-CVPGVG-NH_2	Low ionomer-binding	Valine (V)	571.69
Ac-CVPGKG-NH_2	High ionomer-binding	Lysine (K)	600.73

Peptide design

The peptide sequences in this study consist of one short elastin-like peptide sequence of CVPGXG with an N-terminal cysteine (C) residue for attachment to gold via a thiol bond, and a guest residue X. To test the hypothesis that C was the anchor of the peptide on gold, one peptide was made without a C residue and compared to another identical peptide with a C residue. To test the hypothesis that elastin-like peptides could be designed to bind to ionomer via an ionic bond, two peptides were created. One peptide was designed to bind to the negatively charged the sulfonate groups in the ionomer with a positively charged guest residue (lysine, K). The other peptide served as a control, and was designed such that it did not contain a charged guest residue (valine, V), thus would not have a high affinity for the negatively charged ionomer. The ends of the peptides were acylated and amidated to isolate the effect of the guest residue. The full amino acid sequences are shown in Table 1. Peptides were ordered from GenScript at a purity of 97.6%.

Quartz crystal microbalance with dissipation

A quartz crystal microbalance with dissipation (QCM-D, Q-Sense Explorer, controlled by Q-Soft integrated software from Biolin Scientific) was used to investigate binding behavior of peptides and Nafion® to a gold surface in aqueous solutions. All flow rates were 150 μL/min unless otherwise noted, and all experiments were performed at 18°C. The gold coated sensor (QSX 301, 5 MHz, Biolin Scientific) was cleaned by treatment with an ultraviolet (UV) light/ozone generator (PSD Series, Novascan) for 15 minutes then placing sensor in 20 mL piranha solution (a 5:1:1 mixture of DI water, 25% ammonium hydroxide and 30% hydrogen peroxide, heated to 75℃) for 5 minutes. After piranha treatment, the sensor was rinsed with DI water, dried in N_2, UV/ozone treated again for 15 minutes. The cleaned sensor was mounted in the QCM-D flow module for further rinsing. To rinse, 20 mL of 2% sodium dodecyl sulfate solution was pumped past the sensor, followed by 100 mL DI water. For experimentation, DI water served as the baseline and was pumped past the sensor first. After no appreciable frequency shifts (below 0.5 Hz in 10 minutes) were observed, a peptide solution of 10 μg/mL was introduced into the QCM-D flow module to bind the peptide to the sensor, unless otherwise noted. Frequency and dissipation changes were monitored with time. After the system reached equilibrium, the sensor was rinsed with DI water for approximately 10 minutes to remove any loosely-bound peptide. Then, a 20 μg/mL ionomer (Nafion®) solution was pumped into the chamber until the frequency stabilized. Afterwards, DI water was pumped for 20 minutes to rinse the sensor of loosely-bound ionomer. The third overtone (15 MHz) was used in data analysis. Other control experiments deviating from this protocol are noted in the Results Section. All experiments were performed in triplicate (n=3), unless otherwise noted.

X-ray photoelectron spectroscopy

X-ray photoelectron spectroscopy (XPS) experiments using a PHI Versaprobe 5000 on gold QCM-D sensors with films of CVPGKG peptide alone, and films with CVPGKG peptides attached to Nafion®. A monochromatic Al Kα X-ray source (hv = 1486.6 eV) was operated. Survey scans were performed with an X-ray size of 200 μm in diameter and an analyzer pass energy of 93.9 eV. All of the XPS data were collected at a nominal photoelectron takeoff angle of 0°. The takeoff angle was defined as the angle between the surface normal and the axis of the analyzer lens. The peptide/ionomer coated gold sensors were prepared in the same way as QCM-D experiments. After film assembly in the QCM-D samples were removed from the flow module, rinsed with DI water and dried in N_2 prior to analysis via XPS.

Atomic force microscopy

The surface morphology of Nafion® films assembled on gold sensors via the CVPGKG peptide in the QCM-D was investigated by atomic force microscopy (AFM, Dimension 3100, Veeco Digital Instruments by Bruker, U.S.A.) in tapping mode, mapping both topography and phase simultaneously. Silicon probes (NCHV-A, Bruker, U.S.A.) with silicon tips of a nominal radius of 8 nm, a nominal spring constant of 40 N/m and a resonant frequency of 328 kHz were used. All images were collected with scan rates between 0.5 and 1 Hz, image resolution of 512×512 pixels and scan size of 500×500 nm^2. Samples were prepared as described in the QCM-D section, rinsed by DI water after taking them out of flow module, dried in N_2 and placed into the AFM chamber under atmospheric pressure at room temperature and tested in air. Software (NanoScope Analysis V 1.50, Bruker, U.S.A.) was used for all AFM analysis and image processing. AFM analysis was performed on two samples (n=2).

Fourier-transform infrared spectroscopy

The secondary structure of a CVPGKG peptide monolayer on a gold sensor was analyzed by Fourier-transform infrared spectroscopy. The monolayer was formed on a gold sensor via QCM-D and analyzed on a Nicolet iS50 spectrometer from Thermo Fisher Scientific, with a VeeMAX-II grazing angle accessory (α=80°) that was equipped with a wire grid ZnSe polarizer and an MCT-A detector. Both the accessory and spectrometer were purged with nitrogen. Background spectra (2000 scans) were taken of a bare gold sensor, and subtracted from spectra taken with the peptide monolayer (1200 scans).

Dynamic light scattering

Particle aggregation behavior of elastin-like peptides and ionomer in solution was performed using dynamic light scattering (DLS, DynaPro NanoStar on software Dynamics 7.1.9, measurement range 0.2 to 2500 nm), at a scattering angle of 90° and a fixed wavelength of 662 nm. Dynals analysis is used to obtain hydrodynamic radius. The two peptide solutions outlined in Table 1 (1 mg/mL in DI water) were analyzed alone, as well as in the presence of Nafion®. The concentration of Nafion® ionomer was set at a 1:1 molar ratio of acid group to peptide for each solution. All tests were performed at 25 ℃. Experiments were performed in triplicate (n=3).

Circular dichroism

Circular dichroism (CD) spectroscopy was used to determine the secondary structure of the elastin-like peptide alone and in the presence of ionomer (150 μg/mL peptide and a 1:1 molar ratio of peptide to Nafion® acid group in DI water). Scans were performed on a Jasco J-815 circular dichroism spectrometer at 20°C using a 0.1 cm path length, with 0.5 nm data pitch, a bandwidth of 1.0 nm, scanning speed of 10 nm/min and 5 accumulations. The baseline was DI water.

Statistical analysis

Data from DLS and the QCM-D are represented as the mean ± the standard deviation. Statistical significance was determined by t-test. A threshold value of $\alpha = 0.05$ was chosen, and a p-value at or below 0.05 indicated significance.

Results

Quartz crystal microbalance with dissipation binding analysis

Binding analysis of the peptides to a solid gold surface and ionomer was conducted using QCM-D (Fig. 1). In this technique, negative relative frequency shifts ($\triangle f$) mean the sensor is gaining mass, while positive shifts mean the sensor is losing mass. While Fig. 1 A and B show representative QCM-D data, Supplemental Information (SI) contains data from all of the repeats performed for each QCM experiment (Fig. S1-S2) and control tests (Fig. S3-S5). Shifts in dissipation provide information about mechanical properties. No significant shifts in dissipation are detected in this study, and thus are not shown in Fig. 1, but can be found in the Supplemental Information.

Fig. 1 A-B shows representative frequency monitoring experiments, with arrows indicating when a new solution is introduced to the gold sensor. Briefly, DI water serves as the baseline before introducing peptide solutions. DI water is used to rinse loosely-bound peptide before a Nafion® solution is introduced. All sensors are subjected to a final DI rinse. A control test was conducted where Nafion® was added to the system after the DI water baseline to observe if Nafion® had a significant affinity for the gold sensor (Fig. S3, n=2). No significant frequency shifts were observed in the control after two repeats, thus an interaction between the peptides and Nafion® could be isolated. An additional control experiment was performed with the peptide VPGKG, which is missing the C residue. Without the C residue, ~6-8X lower frequency shifts were observed compared to peptides which contained the residue (Fig. S4). This confirms that the C residue is responsible for gold binding.

After solutions of CVPGVG (Fig. 1A) and CVPGKG (Fig. 1B) are added to the system, statistically similar negative frequency shifts of 6.81 ± 0.68 and 6.42 ± 1.31 Hz are observed, respectively. Negligible shifts in frequency are observed after the DI water rinse for each peptide, indicating a

stable attachment of the C residue to gold. After subsequent Nafion® addition, no significant frequency change is observed for sensors with immobilized CVPGVG peptide, indicating no significant binding between CVPGVG peptide and ionomer (Fig. 1A). Conversely, for sensors with immobilized CVPGKG peptide, ionomer addition resulted in a significant negative frequency shift to 12.2 ± 1.5 Hz (Fig. 1B). No significant shifts in frequency were observed after a final DI water rinse, indicating a stable attachment of ionomer to the CVPGKG peptide in DI water.

To investigate if the interaction between peptide and Nafion® ionomer is electrostatic, control experiments (n=2) were performed by replacing DI water with 10 mM NaOH solution (pH=12). After peptide binding on gold surface, ~6X lower or no frequency shift was observed when Nafion® solution was added compared to experiments in DI water (Fig. S5). As the pKa of lysine is around 10.5, at pH 12 lysine should no longer be protonated. Therefore, this experiment supports the hypothesis that the interaction between peptide and Nafion® is electrostatic.

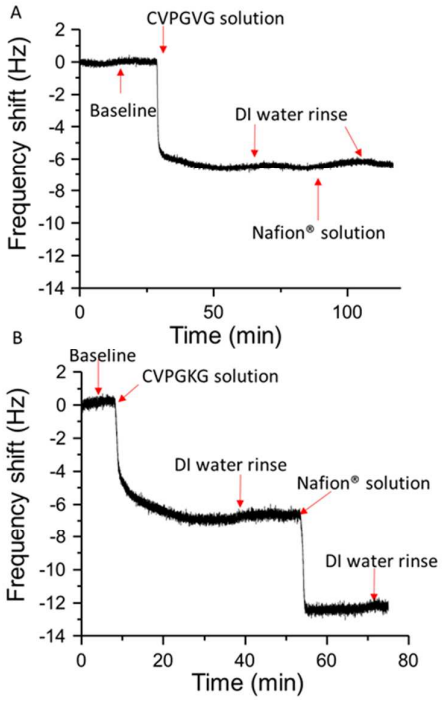

Fig. 1 QCM-D monitoring shows that gold-bound elastin-like peptides can be engineered to bind to ionomer via a K guest residue. (A) Frequency monitoring of CVPGVG peptide and Nafion® ionomer on a gold sensor. (B) Frequency monitoring of CVPGKG peptide and Nafion® ionomer on a gold sensor.

Fig. 2 shows the estimated mass and thickness of the layers based on the frequency monitoring data represented in Fig. 1. The Sauerbrey equation was used to estimate mass and calculate thickness, since small or insignificant dissipation changes were observed, and indicated that films are not viscoelastic, which would violate the assumptions of the model.[29] Additionally, with layers of sufficient thinness (<40 nm) that the Sauerbrey equation is a valid model.[30] Further explanation of the data reduction to obtain mass and thickness estimates be found in Supplemental Information. The negative frequency shifts when peptide solutions are added to the sensor correspond to loadings of 130 ± 26 and 114 ± 23 ng/cm^2 for CVPGVG and CVPGKG peptides respectively (Fig. 2A). The mass values are not statistically different from each other, which means the loading of both peptides is the same on the gold sensors. For sensors with immobilized CVPGKG peptide, Nafion® addition resulted in a significant negative frequency shift to 12.2 ± 1.5 Hz (Fig. 1B), which corresponds to a total mass of 219 ± 26 ng/cm^2 (Fig. 2A). This mass increase is statistically significant compared to the initial mass with just the peptide, which suggests a significant interaction between CVPGKG peptide and the ionomer

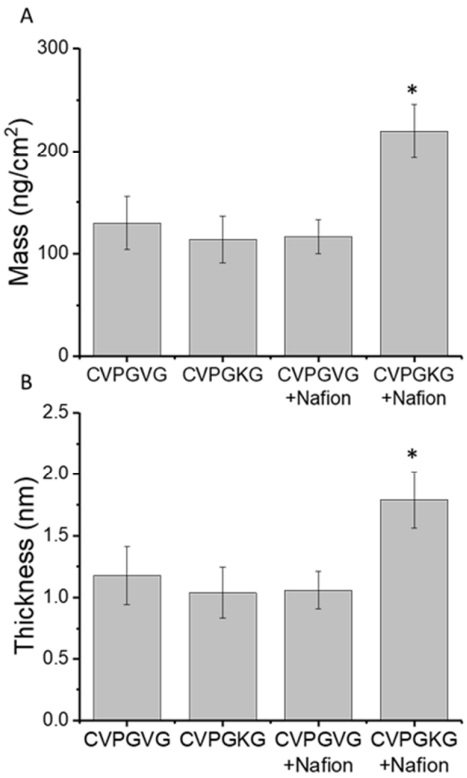

Fig. 2 Mass and thickness estimates of layers created in QCM-D monitoring experiments. (A) Mass calculated from the frequency shifts in Fig. 1 showing the loading of each peptide, and the total mass when Nafion® is added to the sensors with immobilized peptide. (B) Thickness calculated from the frequency shifts showing the estimated thickness of the peptide layers, and the total thickness when Nafion® is added to the sensors with immobilized peptide. (*) represents $p < 0.05$ compared to CVPGKG peptide loading without ionomer, two-tailed t-test, n=3.

(Nafion®) exists. Additionally, when performed on a molar basis, this analysis reveals the loading for the CVPGVG and CVPGKG peptides was 0.23 ± 0.04 and 0.19 ± 0.04 nmol/cm^2 respectively. In the presence of CVPGKG peptide, Nafion® adhered to the sensor such that 0.096 ± 0.004 nmol of acid group/cm^2 were present after binding and a final DI water rinse. Thus, based on the molar analysis, the immobilized CVPGKG

peptide binds in a 2:1 molar ratio of peptide to acid group in Nafion® ionomer.

Thickness is estimated to be 1.18 ± 0.23 and 1.04 ± 0.20 nm for CVPGVG and CVPGKG respectively. When the sensor with immobilized CVPGKG is exposed to ionomer, a significantly thicker layer forms that is approximately 1.79 ± 0.23 nm. These values are discussed in the context of monolayer formation and compared to previous literature results in the Discussion Section.

Surface analysis of peptide-ionomer films using atomic force microscopy, X-ray photoelectron spectroscopy, and Fourier-transform infrared spectroscopy

Atomic force microscopy (AFM), X-ray photoelectron spectroscopy (XPS), and Fourier-transform infrared spectroscopy (FTIR) were utilized to further characterize the CVPGKG and Nafion® films on the gold QCM sensors. XPS was used to confirm the presence of Nafion® on the surface of the gold sensors by comparing peptide-only sensors with the sensors which contained peptide and were exposed to ionomer. The sensor containing CVPGKG which was exposed to the Nafion® solution produced a fluorine peak, whereas the sensor with only peptide did not (Fig. S6). Additionally, both scans revealed the presence of protein material (carbon, nitrogen and oxygen) supporting the presence of the peptide on the sensors as well.

FTIR was used to analyze the secondary structure of the bound peptide monolayer on the gold sensor. FTIR data showed a clear adsorption peak at 1679 cm^{-1} (Fig. S8) indicating the presence of a β-turn structure.[31]

AFM was used to analyze sensor surfaces after thin films were assembled via QCM. Fig. 3 shows the topography and phase images obtained for a bare gold sensor, a gold sensor with the CVPGKG peptide, and a gold sensor with the CVPGKG and Nafion®. Topography images reveal the nature of the bare gold surface to be characterized by round high points surrounded by lower valleys. This general topography doesn't appear to change when peptides are added, and the underlying topography is still similar when ionomer is present with immobilized peptides, however, new circular features appear over the original topography in the samples with Nafion® (Fig. 3C topography, one feature is marked with a white dash arrow). When the same sample is analyzed for phase, it becomes apparent that these overlying features correspond to high phase angle (Fig. 3C phase, one bright region marked with a white dash circle). These are typically associated with hydrophilic regions, while the dark regions with the low phase angles are associated with hydrophobicity.[32-34] The image indicate that a layer of phase separated Nafion® ionomer has formed on the peptide-functionalized gold sensor. Repeat AFM tests showing these phenomena are shown in Fig. S7.

Analysis of peptide and ionomer in solution using dynamic light scattering and circular dichroism

Dynamic light scattering (DLS) which measures hydrodynamic radius, was used to analyze the interactions

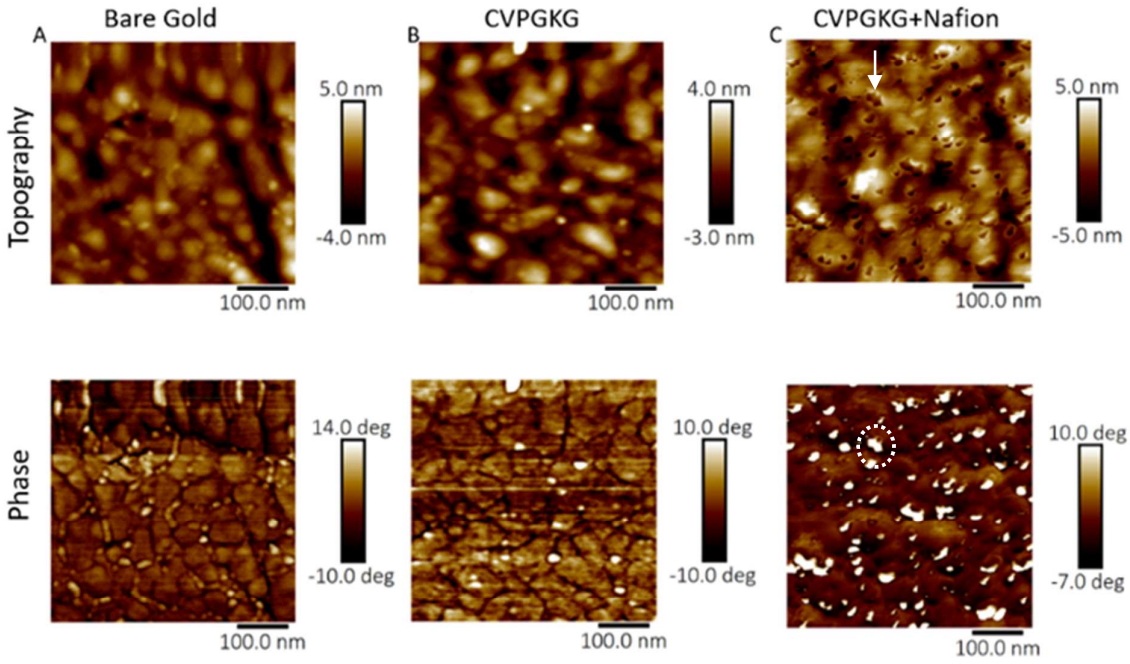

Fig. 3 AFM images show elastin-like peptide is capable of organizing ionomer in to phase-separated regions on gold surfaces. Topography (top panel) and phase angle (bottom panel) are shown for (A) bare gold, (B) gold with immobilized CVPGKG peptide, and (C) Nafion® attached to immobilized CVPGKG peptide. Images are 500 x 500 nm. White dash arrows point to new topographical features observed in samples with a Nafion® layer, and white dash circles show corresponding areas of high phase angle (hydrophilic phase).

Soft Matter

Paper

between peptides and ionomer in solution (Fig. 4). Solutions containing CVPGVG and CVPGKG contained particles with a hydrodynamic radius of 0.61 ± 0.05 nm and 0.75 ± 0.32 respectively. A significant hydrodynamic radii increase to 5.10 ± 0.56 nm was observed in solution containing CVPGKG peptide and Nafion®, but this increase was not observed for the control peptide CVPGVG. The results corroborate the QCM-D binding analysis, which showed a significant interaction between immobilized CVPGKG peptide and acidic ionomer, and shows

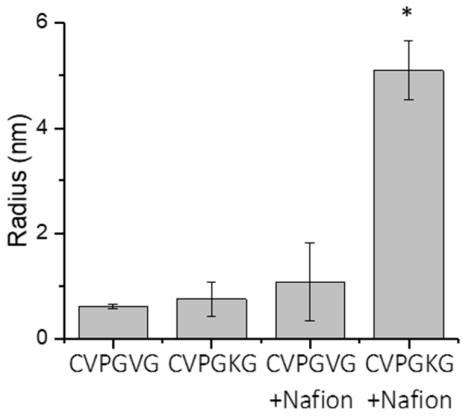

Fig. 4 Demonstration of interactions between engineered elastin-like peptides and Nafion® ionomer in solution. A significant hydrodynamic radius increase was observed when CVPGKG peptide was in the presence of ionomer, but an increase is not observed for solutions with CVPGVG and ionomer. (*) represents $p < 0.05$ compared to solutions without ionomer, two-tailed t-test, n=3.

an interaction also takes place in solution. Dynamic light scattering typically cannot be used to analyze Nafion® ionomer alone in aqueous environments as the ionomer is not truly dissolved.[26] Therefore, a separate size population of Nafion® alone is not observed in the solutions.

The effect of Nafion® ionomer on the secondary structure of the elastin-like peptides was analyzed using CD (Fig. 5). The two peptides were qualitatively analyzed alone in solution, and in the presence of same molar ratio of Nafion® acidic groups in solution. The elastin-like peptide CD spectra showed characteristic features such as a strong negative peak at 197 nm and a less-pronounced minimum at 218 nm.[16] Comparing the results in the presence of Nafion®, the CD spectra had the same peaks, which nearly overlap the alone peptide spectra, indicating the secondary structure remained unchanged. The Nafion® ionomer solution was tested alone as well, and the CD spectra showed no peaks, as expected. The results suggest that the CVPGVG and CVPGKG peptides maintain their secondary structure in presence of Nafion® ionomer.

Discussion

The QCM and DLS results can be used to analyze monolayer formation of the elastin-like peptides on gold surface. The analysis of QCM data reveals that peptides CVPGVG and CVPGKG bind to gold surfaces with statistically similar packing density ($1.37 \pm 0.27 \times 10^{14}$ molecules/cm^2, and $1.14 \pm 0.23 \times 10^{14}$ respectively, using the molecular weights shown in Table 1). While the packing density for these specific elastin-like peptides has not been previously characterized, it is comparable to a QCM study of self-assembled monolayers on gold utilizing a C residue,

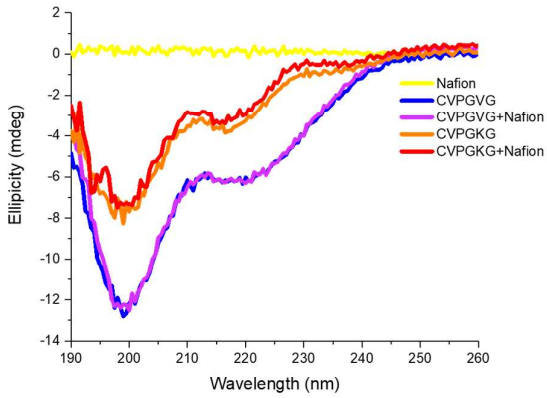

Fig. 5 Elastin-like peptides maintain their secondary structure in the presence of Nafion® ionomer. CD spectra of CVPGVG (blue) and CVPGKG (orange) alone in DI water, and in the presence of ionomer (purple and red, respectively). Nafion® ionomer shows no peaks in CD spectroscopy (yellow).

where a peptide of molecular weight 1851 g/mol was immobilized at a density of 1.2×10^{14} molecule/cm^2.[35] In the same study, the average cross-section of each peptide was ~0.8 nm^2, which indicated dense packing. By the same analysis, the peptides in our study also exhibit dense packing, with a 0.75 ± 0.13 and 0.90 ± 0.19 nm^2 cross-section for a single CVPGVG and CVPGKG peptide, respectively. Interestingly, the K residue did not appear to cause statistically significant steric hindrance and did not limit packing compared to the peptide with a V guest residue. The cross-sectional area estimated from QCM is comparable to the area calculated from the hydrodynamic radius from DLS (1.2 ± 0.2 nm2 and 2.0 ± 1.7

and for CVPGVG and CVPGKG respectively) which validates these estimates by QCM and the model used to calculate mass loading. The QCM and DLS data match a rough size estimate of single peptide, assuming that each amino acid is ~0.35 nm long and peptides are 6 amino acids in length (~0.7 nm), and suggest that a single monolayer is formed on the gold surface. Thickness values calculated from QCM data also have values which correspond to estimated DLS diameters of peptides in solution. The thickness is estimated to be 1.18 ± 0.23 and 1.04 ± 0.20 nm for CVPGVG and CVPGKG respectively for QCM, and diameters measured by DLS are 1.2 ± 0.1 nm and 1.5 ± 0.6, respectively. These values agree with molecular models of similar short elastin-like peptides which would place end residues of our peptide ~0.7-1.2 nm apart when in a β-turn conformation, the structure supported by our CD measurements (Fig. 5)[36] and FTIR data (Fig. S8). In this model, the distance between the ends depended on the low-temperature expanded (~1.2 nm) versus high-temperature contracted (~0.7 nm) state of the peptide.

Only the peptide with K in the guest residue was found to have an interaction with Nafion®, both when immobilized on a metal surface (Fig. 1 and 2) and in solution (Fig. 4). Because this interaction does not occur when V is in the guest residue, and K possesses the only charged amine in the peptide, it is likely that ionic crosslinking is responsible for the interaction. Experiments in pH 12 solution further support the hypothesis that the nature of the interaction between the lysine guest residue and the Nafion® is electrostatic (Fig. S5). It has been shown previously that the sulfonic acid groups in Nafion® will interact with amine groups.[27, 28] This study shows for the first time that the interaction can occur when the amine is part of a peptide chain. It also shows that peptides can be utilized to encourage ionomer binding to metals which normally would have low affinity. Interestingly, the QCM analysis estimates the combined CVPGKG and Nafion® layers are 1.79 ± 0.23 nm thick, whereas in DLS larger aggregates with a hydrodynamic radius of 5.10 ± 0.56 nm are observed. We speculate that the difference in scale may be due to hierarchical structures forming in solution, since both peptide and ionomer are present and have the ability to build multi-layers, where as in the QCM, only one component is exposed to the surface at a time. The discrepancy may also be due to the fact that the hydrodynamic radius from DLS is calculated under the assumption that the particles are spheres, and the peptide-ionomer aggregates may not be spherical in shape. Another interesting observation seen in the DLS data is that Nafion® ionomer alone in aqueous environments is not truly dissolved and unable to be analyzed via DLS,[26] therefore the increase in hydrodynamic radius in the presence of CVPGKG, but not CVPGVG, suggests that the bound peptide-ionomer structure is more soluble than the ionomer alone.

The AFM scan of a QCM sensor functionalized with CVPGKG and Nafion® (Fig. 3) shows distinct areas of phase separation. A recent review of PFSA ionomer understanding which includes analysis of nanomorphology as well as thin film behavior provides context for these results. Notably, transmission electron microscopy has been used to visualize dry bulk PFSA films and has shown circular phase separated nanostructures of 3 to 8 nm, where the circular regions are hydrophilic, similar to results in this study.[37] However, generally, as the thickness of PFSA films decreases below an ultrathin regime of 15-20 nm, films exhibit dispersion-like behavior with weak phase separation between hydrophilic and hydrophobic domains. While metal substrate properties influence the thickness of this regime, this weak phase separation behavior has been observed on gold in thicknesses <20 nm.[38] Therefore, the observation of phase separation within this ultrathin regime on gold demonstrates the potential utility of peptide engineering in organizing ionomer layers.

In this study, short elastin-like peptides were chosen for their many attractive properties as outlined in the introduction. One property that is of potential interest is the secondary structure of elastin, as it may be useful in future studies which investigate control over self-assembly or conformational changes to environmental stimuli. As the QCM studies show, the structure and/or orientation of the peptide when immobilized to a gold surface via a thiol-bond does not inhibit the binding of the K residue to Nafion® ionomer. Secondary structure analysis using CD was performed to investigate what the structure is in solution, and in the presence of Nafion® (Fig. 5). The two elastin-like peptides exhibited a strong negative peak at 197 nm and a less-pronounced minimum at 218 nm. In previous studies with similar short ELPs, these two minimum and spectral shape are typical.[16, 36] The peaks at 218 and 197 nm point to structural features of elastin-like peptides, which are for random coil and β-turn structures, respectively.[39] Spectra of the peptides alone are similar to previous results obtained by Nuhn *et al.* showing a higher proportion of random coil compared to β-turns in a short elastin peptide sample (GVGVPGVG) at room temperature.[16] Comparing the CD specta between peptide alone and peptide in the presence of Nafion® solution, the spectra are overlap with each other, indicating the secondary structures of the two elastin-like peptides remain unchanged at the concentrations studied in the presence of the acidic ionomer. While this particular system (elastin-like peptide with Nafion® ionomer) has not been studied previously, the stability of elastin in acidic polyelectrolytes has been demonstrated, as elastin sequences have been incorporated with polyacrylic acid (PAA) to form highly stable nanostructures for biomedical applications.[40] Additionally, FTIR data showed that the CVPGKG peptide exhibited some β-turn secondary structures even after binding to the metal surface, which indicates the unique properties of self-assembly and environmental sensitivity could be exploited in the future to control ionomer on metal surfaces.

Conclusions

Short elastin-like hexapeptides (CVPGVG and CVPGKG) were designed to bind to gold via a cysteine residue, and formation of peptide monolayers on gold was observed. The hexapeptide containing a lysine guest residue bound to Nafion® ionomer which happened when the peptide was

immobilized on gold, as well as in solution. This peptide facilitated the formation of a thin, phase separated ionomer layer on a gold surface, and the peptide maintained its characteristic secondary structure when attached to gold and in the presence of Nafion® ionomer in solution. Generally, these results show that protein sequences can be utilized for ionomer organization, which has applications in the electrochemical fields of sensing, enzyme-based catalysis, and energy conversion. Current and future work will study the effect of elastin peptide composition and length on the organization and phase separation of ionomer thin films on metal surfaces, and ability to respond to environmental stimuli.

Conflicts of interest

There are no conflicts to declare.

Acknowledgements

This work was supported by the Electrochemical Society Young Investigator Fellowship which was awarded to Julie N. Renner, and a National Science Foundation-sponsored Research Experiences for Undergraduates Award (Award Number 1659394) which funded co-author Skylar Watson. We appreciate the assistance from the Swagelok Center for Surface Analysis of Material located at Case Western Reserve University for their work in helping obtain AFM and XPS data. We also thank Dr. Yinghua Chen and the Protein Expression Purification Crystallization and Molecular Biophysics Core of Case Western Reserve University Department of Physiology and Biophysics for assistance with DLS measurement, and Dr. Smarajit Bandyopadhyay at the Case Western Reserve University Molecular Biotechnology Core Facility for assistance with CD. Finally, we thank the kind contributions of Matt Bartucci at Thermofisher for gathering the FTIR data.

References

1. J. N. Renner and S. D. Minteer, *Experimental Biology and Medicine*, 2016, **241**, 980-985.
2. A. K. Sarma, P. Vatsyayan, P. Goswami and S. D. Minteer, *Biosensors & Bioelectronics*, 2009, **24**, 2313-2322.
3. M. Rasmussen, S. Abdellaoui and S. D. Minteer, *Biosensors & Bioelectronics*, 2016, **76**, 91-102.
4. H. Wang, Y. Yang and L. Guo, *Advanced Energy Materials*, 2017, **7**, 18.
5. W. Wang, C. F. Anderson, Z. Y. Wang, W. Wu, H. G. Cui and C. J. Liu, *Chem. Sci.*, 2017, **8**, 3310-3324.
6. A. Z. Weber and A. Kusoglu, *Journal of Materials Chemistry A*, 2014, **2**, 17207-17211.
7. Q. He, N. S. Suraweera, D. C. Joy and D. J. Keffer, *The Journal of Physical Chemistry C*, 2013, **117**, 25305-25316.
8. S. M. Andersen, *Appl. Catal. B-Environ.*, 2016, **181**, 146-155.
9. C. M. Moore, N. L. Akers, A. D. Hill, Z. C. Johnson and S. D. Minteer, *Biomacromolecules*, 2004, **5**, 1241-1247.
10. N. L. Akers, C. M. Moore and S. D. Minteer, *Electrochimica Acta*, 2005, **50**, 2521-2525.
11. S. Meredith, S. Xu, M. T. Meredith and S. D. Minteer, *J. Vis. Exp.*, 2012, DOI: 10.3791/3949, 6.
12. D. W. Urry, T. L. Trapane and K. U. Prasad, *Biopolymers*, 1985, **24**, 2345-2356.
13. D. W. Urry, C. H. Luan, T. M. Parker, D. C. Gowda, K. U. Prasad, M. C. Reid and A. Safavy, *J. Am. Chem. Soc.*, 1991, **113**, 4346-4348.
14. D. E. Meyer and A. Chilkoti, *Biomacromolecules*, 2004, **5**, 846-851.
15. D. J. Callahan, W. Liu, X. Li, M. R. Dreher, W. Hassouneh, M. Kim, P. Marszalek and A. Chilkoti, *Nano Letters*, 2012, **12**, 2165-2170.
16. H. Nuhn and H. A. Klok, *Biomacromolecules*, 2008, **9**, 2755-2763.
17. M. Shimazu, A. Mulchandani and W. Chen, *Biotechnol. Bioeng.*, 2003, **81**, 74-79.
18. G. L. Guo, T. H. A. Truong, H. T. T. Tan, H. X. Ang, W. Y. Zhang, C. Xu, X. H. Rui, Z. L. Hu, E. Fong and Q. Y. Yan, *Chem.-Asian J.*, 2014, **9**, 2555-2559.
19. J. Reguera, A. Fahmi, P. Moriarty, A. Girotti and J. C. Rodriguez-Cabello, *J. Am. Chem. Soc.*, 2004, **126**, 13212-13213.
20. D. E. Meyer and A. Chilkoti, *Nat. Biotechnol.*, 1999, **17**, 1112-1115.
21. G. Guo, X. Yao, H. Ang, H. Tan, Y. Zhang, Y. Guo, E. Fong and Q. Yan, *Nanotechnology*, 2016, **27**.
22. Y. Lu, Y. P. Zhou, Q. Y. Yan and E. Fong, *Journal of Materials Chemistry A*, 2016, **4**, 2691-2698.
23. Y. Lu, H. Ang, Q. Yan and E. Fong, *Chem. Mat.*, 2016, **28**, 5743-5752.
24. B. A. Paik, M. A. Blanco, X. Q. Jia, C. J. Roberts and K. L. Kiick, *Soft Matter*, 2015, **11**, 1839-1850.
25. C. A. Weeks, B. Aden, S. M. Kilbey and A. V. Janorkar, *ACS Biomaterials Science & Engineering*, 2016, **2**, 2196-2206.
26. K. A. Mauritz and R. B. Moore, *Chem. Rev.*, 2004, **104**, 4535-4585.
27. W. F. Chen, Y. C. Shen, H. M. Hsu and P. L. Kuo, *Polym. Chem.*, 2012, **3**, 1991-1995.
28. W. F. Chen and P. L. Kuo, *Macromolecules*, 2007, **40**, 1987-1994.
29. M. C. Dixon, *Journal of Biomolecular Techniques : JBT*, 2008, **19**, 151-158.
30. B. D. Vogt, E. K. Lin, W. L. Wu and C. C. White, *J. Phys. Chem. B*, 2004, **108**, 12685-12690.
31. A. Barth, *Biochim. Biophys. Acta-Bioenerg.*, 2007, **1767**, 1073-1101.
32. A. Ohira, S. Kuroda, H. F. M. Mohamed and B. Tavernier, *Phys. Chem. Chem. Phys.*, 2013, **15**, 11494-11500.
33. M. L. Einsla, Y. S. Kim, M. Hawley, H. S. Lee, J. E. McGrath, B. J. Liu, M. D. Guiver and B. S. Pivovar, *Chem. Mat.*, 2008, **20**, 5636-5642.
34. R. S. McLean, M. Doyle and B. B. Sauer, *Macromolecules*, 2000, **33**, 6541-6550.
35. J. Wu, J. P. Park, K. Dooley, D. M. Cropek, A. C. West and S. Banta, *PLoS One*, 2011, **6**, 9.
36. H. Reiersen, A. R. Clarke and A. R. Rees, *J. Mol. Biol.*, 1998, **283**, 255-264.
37. A. Kusoglu and A. Z. Weber, *Chem. Rev.*, 2017, **117**, 987-1104.

38. A. Kusoglu, D. Kushner, D. K. Paul, K. Karan, M. A. Hickner and A. Z. Weber, *Adv. Funct. Mater.*, 2014, **24**, 4763-4774.
39. D. W. Urry, M. M. Long, B. A. Cox, T. Ohnishi, L. W. Mitchell and M. Jacobs, *Biochimica et Biophysica Acta (BBA) - Protein Structure*, 1974, **371**, 597-602.
40. S. E. Grieshaber, B. A. Paik, S. Bai, K. L. Kiick and X. Q. Jia, *Soft Matter*, 2013, **9**, 1589-1599.

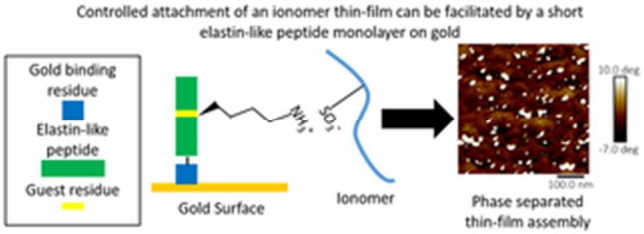

28x10mm (300 x 300 DPI)